Hindawi Publishing Corporation
Conference Papers in Science
Volume 2014, Article ID 684352, 7 pages
http://dx.doi.org/10.1155/2014/684352

Conference Paper

Antibacterial Activity of a Chitosan-PVA-Ag^+-Tobermorite Composite for Periodontal Repair

Andrew P. Hurt, Alejandra A. Ruiz de Clavijo, George J. Vine, Aimee A. Coleman, and Nichola J. Coleman

School of Science, University of Greenwich, Chatham Maritime, Kent ME4 4TB, UK

Correspondence should be addressed to Nichola J. Coleman; nj_coleman@yahoo.co.uk

Received 21 November 2013; Accepted 12 February 2014; Published 7 April 2014

Academic Editors: J. Gough and R. Sammons

This Conference Paper is based on a presentation given by Andrew P. Hurt at "UK Society for Biomaterials Annual Conference 2013" held from 24 June 2013 to 25 June 2013 in Birmingham, United Kingdom.

A polymer-mineral composite was prepared by solvent casting a mixture of chitosan, poly(vinyl alcohol), and Ag^+-exchanged tobermorite in dilute acetic acid and characterised by scanning electron microscopy and Fourier transform infrared spectroscopy. The *in vitro* bioactivity of the CPTAg membrane was confirmed by the formation of hydroxyapatite on its surface in simulated body fluid. The alkaline dissolution products of the tobermorite lattice buffered the acidic breakdown products of the chitosan polymer and the presence of silver ions resulted in marked antimicrobial action against *S. aureus*, *P. aeruginosa*, and *E. coli*. The *in vitro* cytocompatibility of the CPTAg membrane was confirmed using MG63 osteosarcoma cells. The findings of this preliminary study have indicated that chitosan-poly(vinyl alcohol)-Ag^+-tobermorite composites may be suitable materials for guided tissue regeneration applications.

1. Introduction

Periodontitis is an infectious disease that destroys the tooth attachment apparatus. During the progression of the disease, the epithelial tissue detaches from the tooth, the periodontal ligament (PDL) disconnects, and the alveolar bone tissue is resorbed (as shown in Figure 1(a)) [1, 2]. Traditional treatment of periodontitis involves the debridement and cleaning of the root surface without the restoration of the tooth attachment apparatus. Rapidly migrating epithelial cells subsequently grow alongside the tooth root and prevent the reestablishment and reattachment of the PDL and alveolar bone at the defect site. The development of biocompatible membranes for the guided tissue regeneration (GTR) of the periodontal structures is an area of increasing interest in the treatment of periodontitis. GTR strategies involve the placement of a barrier to exclude the epithelial and gingival tissues from the exposed root surface to provide an opportunity for the more slow-growing bone and PDL tissues to regenerate (as shown in Figure 1(b)). Animal models have demonstrated that, in comparison with conventional treatment, resorbable chitosan-based GTR membranes promote the regeneration of the tooth attachment apparatus [3–5]. Improvements in the design of GTR membranes are now sought *via* the incorporation of bioactive and antimicrobial components that enhance tissue regeneration and reduce infection [2].

Chitosan is the partially N-deacetylated derivative of chitin, a linear structural polysaccharide obtained on an industrial scale from the shells of crustaceans [6–8]. It is abundant, readily renewable, biodegradable, bioactive, biocompatible, antibacterial, and nonantigenic. Biomedical applications of chitosan include drug delivery systems; wound dressings and medical textiles; resorbable sutures; and tissue engineering scaffolds [6–13]. The structure of chitosan, a basic copolymer of glucosamine and N-acetylglucosamine, resembles that of glycosaminoglycans which are the principal components of bone extracellular matrix (ECM) [11, 13]. In this respect, chitosan is a popular candidate material for *in situ* periodontal tissue engineering [1–5, 10]. Disadvantages of chitosan in this application are that it is mechanically weak, insufficiently bioactive to effect the required initial rapid bone regeneration and, despite intrinsic bacteriostatic

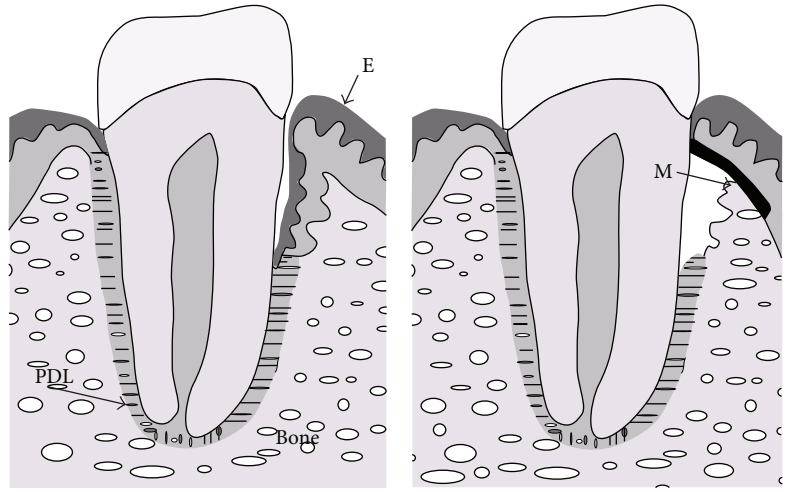

Figure 1: A sketch of (a) periodontal ligament (PDL) detachment and alveolar bone loss during periodontitis and (b) the placement of a GTR membrane (M) to prevent epithelial (E) migration and to stimulate the regeneration of lost bone.

properties, susceptible to biofilm formation. These problems can be addressed by reinforcing the chitosan with antibacterial and osteogenic inorganic phases, such as silver nanoparticles, hydroxyapatite, and bioactive glass, that confer superior microbial resistance, improve mechanical strength, and/or stimulate osteogenesis [10, 12–14]. The mechanical properties of chitosan can also be enhanced by blending with other polymers. Poly(vinyl alcohol) (PVA) is a biocompatible water-soluble synthetic polyhydroxy polymer that has been blended with chitosan to increase its mechanical strength, hydrophilicity, and cytocompatibility [15–17].

Tobermorite, $Ca_5Si_6O_{16}(OH)_2{\cdot}4H_2O$, is a bioactive calcium silicate mineral that exhibits antibacterial activity against both Gram-positive and Gram-negative bacteria when silver ions are exchanged into its lattice [18, 19]. The structure of tobermorite is similar to that of the principal calcium silicate hydrate gel phase of the endodontic cement, ProRoot MTA, which is reported to stimulate the regeneration of cementum and bone tissue [20, 21].

In this study, the authors have prepared a composite GTR membrane of chitosan, PVA, and Ag^+-exchanged tobermorite by solvent casting from dilute acetic acid solution. The composite membrane was characterised by scanning electron microscopy (SEM) and Fourier transform infrared spectroscopy (FTIR). The Kirby-Bauer "zone of inhibition" assay was used to determine the antibacterial activity of the composite membrane against *Staphylococcus aureus*, *Pseudomonas aeruginosa*, and *Escherichia coli*. *In vitro* bioactivity was evaluated by monitoring the formation of hydroxyapatite on the surface of the membrane during immersion in simulated body fluid and an indication of biocompatibility was obtained using MG63 human osteosarcoma cells.

2. Experimental

2.1. Sample Preparation and Characterisation. Low molecular weight chitosan (molecular weight 50–190 kDa, degree of deacetylation 75–85%), PVA (molecular weight 13–23 kDa, degree of hydrolysis 87–89%), and all other reagents were purchased from Sigma-Aldrich, UK, and used without further purification. Tobermorite samples were prepared in triplicate by heating mixtures of 6.8 g of sodium metasilicate pentahydrate, 1.47 g of calcium oxide, and 60 cm^3 of 1.0 M sodium hydroxide solution at 100°C in sealed Teflon reaction vessels for 19 days. The products were washed with deionised water to pH ~7 and dried in air at 40°C to constant mass. Silver-exchanged tobermorite was obtained by exposing 0.5 g of the original tobermorite product to 200 cm^3 of 3.0 mM $AgNO_3$(aq) for 9 days. The Ag^+-exchanged tobermorite was recovered by gravitational filtration, dried in air to constant mass at 40°C, and characterised by powder X-ray diffraction (XRD) analysis and X-ray fluorescence spectroscopy (XRF), as described in [19]. The formula of the Ag^+-exchanged tobermorite used in this study was $Ca_{4.06}Na_{0.04}Ag_{0.92}Si_{6.00}O_{16.54}{\cdot}11.9H_2O$.

Chitosan-PVA-Ag^+-tobermorite (CPTAg) composite membranes were prepared at the mass ratio 75 : 25 : 70 in triplicate by solvent casting. In each case, 0.45 g of chitosan and 0.15 g of PVA were dissolved in 30 cm^3 of 2% (v/v) ethanoic acid solution at room temperature. 0.42 g of Ag^+-tobermorite was added and the mixtures were stirred for 2 hours, cast onto polycarbonate plates, and dried in air at 60°C for 2 days to produce membranes. Control samples (labelled CPT) for the Kirby-Bauer assay were also prepared similarly with the original unexchanged tobermorite. The CPTAg membranes were characterised by FTIR using a Perkin Elmer Paragon spectrometer and SEM using uncoated samples attached to carbon tabs on a Hitachi SU8030 scanning electron microscope. Secondary electron images were obtained at an accelerating voltage of 1 kV.

2.2. Antibacterial Properties of CPTAg and CPT Membranes. The antimicrobial activities of the CPTAg and CPT composite

membranes were evaluated using the semiquantitative Kirby-Bauer inhibition zone method against Gram-positive *Staphylococcus aureus* NCIMB 9518, Gram-negative *Escherichia coli* NCIMB 9132, and Gram-negative *Pseudomonas aeruginosa* NCIMB 8628. In each case, 100 cm^3 of Nutrient Broth (Oxoid) was inoculated with 0.1 cm^3 of an overnight culture of the bacterium. The cultures were then incubated for 24 hours, with shaking, at 37°C. 0.2 cm^3 of the resulting cultures was spread in quadruplicate on nutrient agar plates. 8 mm discs were punched from the CPTAg and CPT composite membranes and one disc was placed in the centre of each spread plate. The plates were examined for clear zones after incubation at 37°C for 24 hours. Plate counts indicated that the final population densities of the plates spread with *S. aureus*, *E. coli*, and *P. aeruginosa* were approximately 1.0×10^9, 5.9×10^8, and 5.9×10^9 colony forming units *per* plate.

2.3. In Vitro Bioactivity of CPTAg Membrane. Simulated body fluid (SBF) was prepared according to the method described by Kokubo and Takadama [22] and stored for no longer than 3 days prior to use. 16 cm^3 sections (approximate mass 40 mg) of CPTAg membrane were contacted with 20 cm^3 of SBF solution in hermetically sealed polypropylene containers at 37°C for time intervals of 3, 7, and 14 days. Each analysis was carried out in triplicate. The pH values of the supernatant liquors were measured using a Jenway 3150 pH meter and the solution concentrations of calcium, phosphorus, and silicon were monitored by inductively coupled plasma (ICP) analysis using a Perkin Elmer Optima 4300 DV spectrophotometer and multielement standards. The CPTAg membranes were recovered from SBF solution, washed with deionised water, dried in air at 37°C for 24 h, and analysed by FTIR.

2.4. In Vitro Biocompatibility of CPTAg Membrane. CPTAg membranes were sectioned into 1 mm by 4 mm strips. In triplicate, either 0, 1, or 2 strips were placed in a 96-well plate and sterilised *via* UV irradiation for 3 hours on each side. MG63 osteosarcoma cells (ECACC code: 86051601) were harvested from a main culture at low-passage (<10) at confluency of 80–90% and >90% viability. They were suspended in fresh media and added to the wells at 10^6 cells cm^{-3} and 0.2 cm^3 total volume. The cells were then incubated for 24 hours at 37°C and 5% CO_2. An MTT (3-(4, 5-dimethyl-2-thiazolyl)-2, 5-diphenyl-2H-tetrazolium bromide) analysis was conducted to evaluate the toxicity of the CPTAg membrane. The absorbance data collected at 540 nm were subjected to a one-tailed t-test at $(n - 2)$ degrees of freedom and $P = 0.05$.

3. Results and Discussion

3.1. Characterisation of CPTAg Membrane. The FTIR spectrum of pure chitosan is shown in Figure 2(a). The broad signal at *ca.* 3460 cm^{-1} arises from N–H and O–H stretching vibrations which overlap in this region [23]. Amide I C=O stretching modes and amide II N–H bending vibrations give rise to the bands at 1650 cm^{-1} and 1570 cm^{-1}, respectively. Aliphatic C–H bending vibrations give rise to the bands at

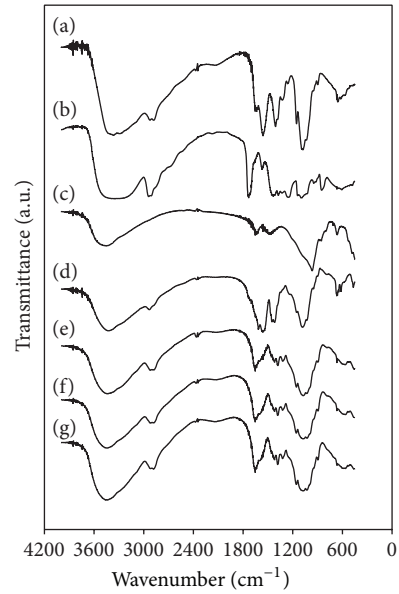

Figure 2: FTIR spectra of (a) chitosan, (b) PVA, (c) tobermorite, (d) composite C-T membrane; and C-T membrane after immersion in SBF for (e) 3 days, (f) 7 days, and (g) 14 days.

1420–1430 cm^{-1} and 1365 cm^{-1}, and C–H stretching frequencies appear at 2960–2965 cm^{-1}. Various C–O–C stretching modes give rise to the signals in the 1160–1060 cm^{-1} region and the band at 1295 cm^{-1} is assigned to C–O–H stretching vibrations.

The FTIR spectrum of pure PVA is shown in Figure 2(b). The very broad signal centered at ~3350 cm^{-1} arises from stretching vibrations of hydrogen-bonded O–H groups along the polymer chain. C–H stretching modes give rise to the band at ~2930 cm^{-1} and the signals at 1720 cm^{-1} and 1100 cm^{-1} are, respectively, attributed to residual unhydrolysed C=O acetate groups and C–O stretching modes [16, 17]. The FTIR spectrum of tobermorite is shown in Figure 2(c). The combination band at ~970 cm^{-1} is assigned to various Si–O stretching modes of the silicate lattice and the sharp band at 675 cm^{-1} arises from Si–O–Si bending vibrations [19]. O–H vibrations of interlayer water molecules and silanol (Si–OH) groups give rise to the broad signals at 3500 cm^{-1} and 1650 cm^{-1}.

The FTIR spectrum of the CPTAg composite membrane, shown in Figure 2(d), is a superposition of the individual spectra of chitosan, PVA, and tobermorite. No significant shifts in the positions of the characteristic bands and no new signals were observed in the spectrum of the CPTAg membrane. SEM micrographs of the CPTAg composite are shown in Figure 3. These micrographs indicate that the surface of the membrane is highly textured and that the original porous network morphology of the embedded Ag^+-tobermorite particles is still "visible."

3.2. Antibacterial Properties of CPTAg and CPT Membranes. The results of the *in vitro* antibacterial Kirby-Bauer assays are listed in Table 1. The composite membranes incorporating

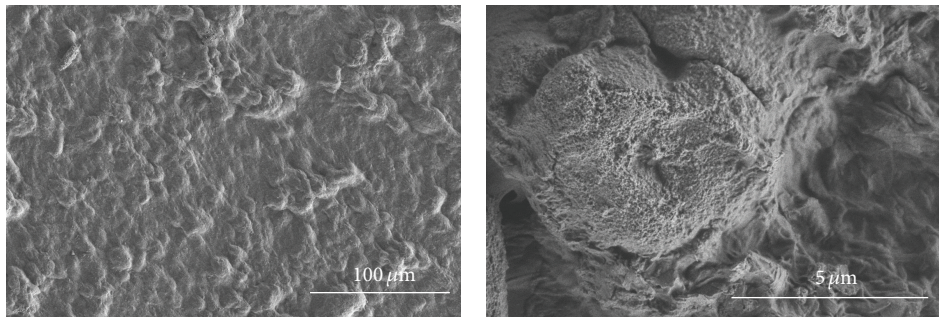

(a) (b)

Figure 3: SEM micrographs of the CPTAg membrane at magnifications of (a) ×1 000 and (b) ×11 000.

Table 1: Inhibition zone data for CPTAg and CPT membranes.

Bacterium	CPTAg	CPT control
E. coli		
Zone of inhibition (mm)	0.89 ± 0.25	0
S. aureus		0
Zone of inhibition (mm)	0.50 ± 0.43	
P. aeruginosa		
Zone of inhibition (mm)	1.40 ± 0.25	0

Ag^+-exchanged tobermorite, CPTAg, exhibited distinct and clear antimicrobial zones against both Gram-positive and Gram-negative bacteria. Conversely, films prepared from the "as synthesized" tobermorite, CPT, failed to exhibit a discrete inhibition zone against any of the bacteria using this method. In fact, in all cases the microbes readily populated the surfaces of the control CPT membrane discs. Images of the CPTAg and CPT membrane discs in contact with *P. aeruginosa* and *E. coli* following an incubation time of 24 hours are presented in Figure 4.

3.3. In Vitro Bioactivity of CPTAg Membrane. The *in vitro* formation of substituted hydroxyapatite, $(Ca,Mg,Na)_{10}(PO_4, CO_3,Cl)_6(OH)_2$, (HA) on the surface of the composite CPTAg membrane was monitored by FTIR spectroscopy and ICP analysis. The FTIR spectra of the CPTAg membrane following exposure to SBF for periods of 3, 7, and 14 days are shown in Figures 2(e), 2(f), and 2(g), respectively, and the corresponding concentrations of calcium, phosphorus, and silicon species in the supernatant solution are plotted in Figure 5. The doublet at 570–610 cm^{-1} arising from phosphate P–O bending modes in the FTIR spectrum of the CPTAg membrane following a residence time of 3 days (Figure 2(e)) is evidence of the formation of crystalline HA on the surface of the sample and the broadening of the combination band centered around 1075 cm^{-1} is attributed to the contribution of P–O stretching modes in the 1000–1220 cm^{-1} region [19]. The concomitant removal of phosphate species from SBF and the release of silicate and calcium species from the tobermorite lattice are shown in Figure 5. It should be noted that the rate of degradation of the silicate lattice in a closed system such as this will be influenced not only by the precipitation of HA on the surface of the material but also more significantly by the solubility limit of silicate species under these experimental conditions. The concentration of phosphate species continues to decrease markedly to below 1 ppm between 3 and 7 days and by 14 days the SBF solution is essentially depleted of phosphate ions (Figure 5) as the precipitation of HA on the surface of the CPTAg membrane continues (Figures 2(f) and 2(g)). Despite the relatively rapid degradation of the tobermorite matrix, the release of silver ions into the SBF solution is comparatively slow. No silver is detected in the supernatant solution after 3 days and only 0.5 ppm is observed after a week. It is possible that silver ions released by the degradation of the Ag^+-tobermorite lattice will undergo ion exchange interactions with the functional groups of chitosan that delay their immediate release into solution.

Throughout the investigation, the pH of the SBF solution fluctuated a little from the original value of 7.45 (Figure 5), indicating that neither the acidic breakdown products of chitosan nor the alkaline dissolution components of the tobermorite lattice significantly affected the pH of the medium.

Visual observation of the CPTAg membranes exposed to SBF solution for 14 days indicated that they remained intact and that they were also mechanically stable during further handling, drying, and analysis.

3.4. In Vitro Biocompatibility of CPTAg Membrane. Cell viability data for MG63 osteosarcoma cells cultured in contact with increasing numbers of CPTAg membrane strips are compared with those of the control (which consisted of cells and medium only) in Figure 6. These data indicate no significant difference between cell viabilities after culturing MG63 cells for 24 hours in contact with the CPTAg membrane strips or the control ($P = 0.05$, $n = 3$). These results suggest that the composite CPTAg membrane does not exert toxicity over human osteoblastic cells.

3.5. CPTAg as a GTR Membrane. Chitosan is a popular candidate material for GTR membranes for periodontal pocket therapy as it is readily available, cost-effective, biocompatible, resorbable, nonantigenic, bioactive, antimicrobial, and is comprised of similar structural units to those of bone ECM [1–5]. Major disadvantages of pure chitosan in this

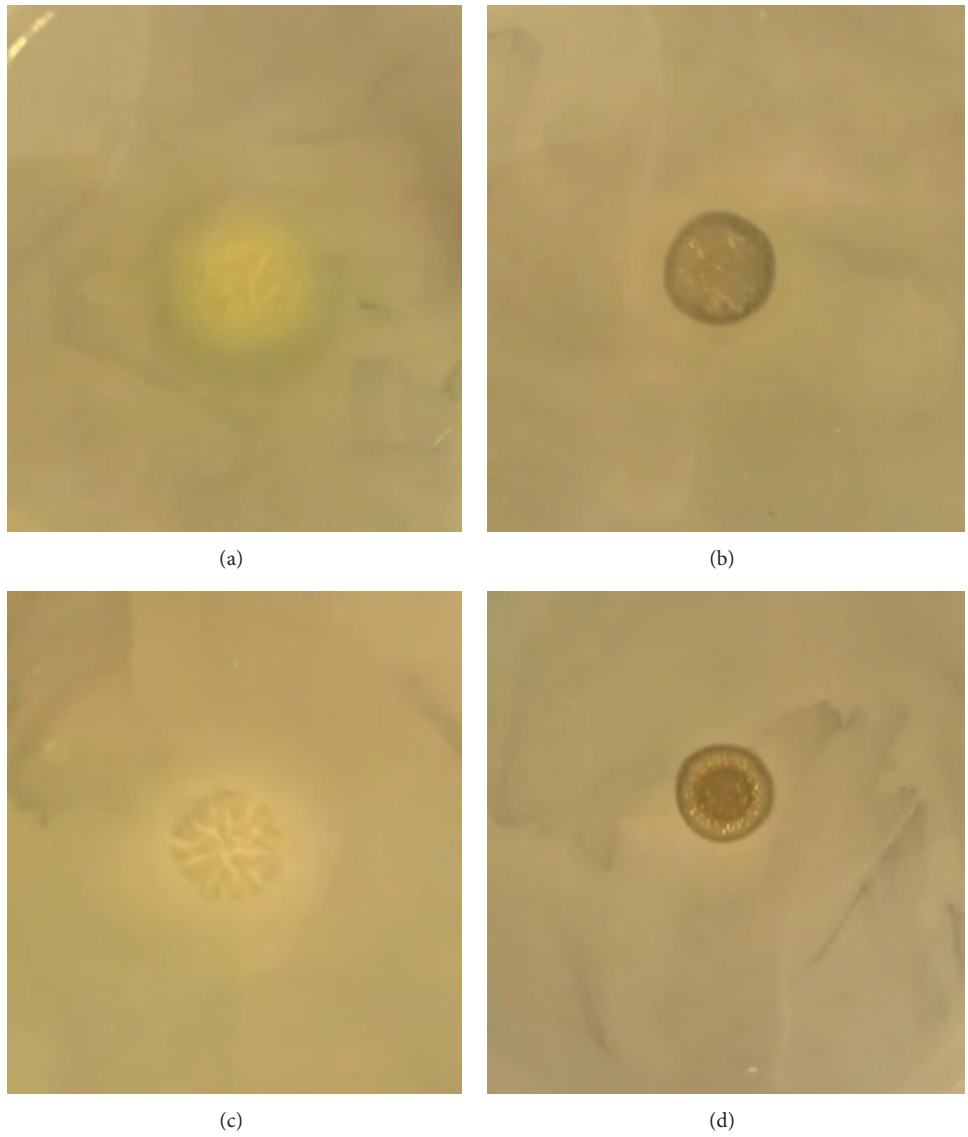

Figure 4: Zone of inhibition images for (a) CPT and *P. aeruginosa*, (b) CPTAg and *P. aeruginosa*, (c) CPT and *E. coli*, and (d) CPTAg and *E. coli*.

application are that its mechanical strength, antimicrobial properties, and bioactivity are insufficient and that its acidic degradation products provoke inflammatory reactions that inhibit healing [23, 24]. The research presented here has demonstrated that degradable, antimicrobial, bioactive, and biocompatible chitosan-PVA-Ag^+-tobermorite composite membranes can be prepared *via* a simple one-step process by solvent casting the components from dilute ethanoic acid solution.

The CPTAg membrane prepared in this study exhibits rapid *in vitro* bioactivity which is principally attributed to the precipitation of HA onto the basic Si–OH nucleation centres presented by the nanoporous silicate layers within the tobermorite lattice [19]. The tobermorite lattice degrades on contact with SBF releasing calcium, silicate, silver, and hydroxide ions into solution. Calcium and hydroxide ions released from the lattice buffer the acidic breakdown products of the chitosan which may mitigate any inflammatory response associated with deviations from physiological pH ~7.45. Dissolved silicate species are known to enhance the production of cytokines and proteins that regulate bone-growth [25, 26], and, in this respect, the release of silicates is likely to confer additional *in vivo* bioactivity on the CPTAg membrane. The presence of silver ions in the composite membrane contributes significantly to its antimicrobial resistance to both Gram-positive and Gram-negative bacteria with no apparent compromise in cytocompatibility. The slow release of silver ions from the CPTAg composite may also be advantageous, as it is envisaged that the sustained antimicrobial activity of the membrane will reduce bacterial biofilm formation.

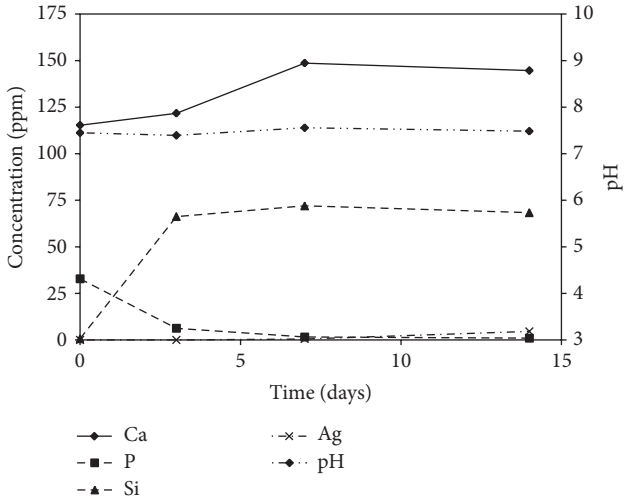

Figure 5: Concentrations of P, Ca, and Si in SBF and corresponding pH as functions of CPTAg residence time in SBF.

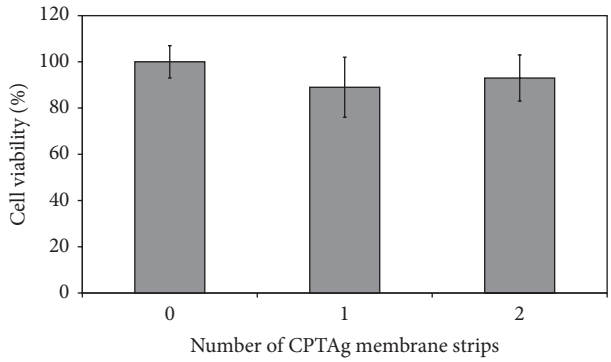

Figure 6: MTT cytocompatibility assay data for MG63 human osteosarcoma cells in contact with CPTAg membranes.

This initial study has shown that chitosan-PVA-Ag^+-tobermorite composite membranes are potential candidate materials for guided tissue regeneration of periodontal defects. Further work is now underway to optimise the formulations with respect to their mechanical properties, resorption rates, osteogenic behavior, and broad-spectrum antimicrobial activity.

4. Conclusions

A polymer-mineral composite, CPTAg, was prepared *via* a simple one-step process by solvent casting a mixture of chitosan, poly(vinyl alcohol), and Ag^+-exchanged tobermorite in dilute acetic acid. The antimicrobial properties, bioactivity, and biocompatibility of the resulting composite membrane were assessed with respect to its application as a guided tissue regeneration (GTR) membrane for periodontal pocket repair. The *in vitro* bioactivity of the CPTAg membrane was confirmed by the formation of hydroxyapatite on its surface in simulated body fluid (SBF). The tobermorite lattice began to degrade on contact with SBF releasing calcium, silicate, silver, and hydroxide ions. The alkaline degradation products buffered the acidic breakdown products of the chitosan polymer and the presence of silver ions resulted in marked antimicrobial action against *S. aureus*, *P. aeruginosa*, and *E. coli*. The cytocompatibility of the CPTAg membrane was confirmed using MG63 osteosarcoma cells (*via* MTT assay). The findings of this preliminary study have indicated that chitosan-poly(vinyl alcohol)-Ag^+-tobermorite composites are promising materials for GTR.

Conflict of Interests

The authors declare that there is no conflict of interests regarding the publication of this paper.

References

[1] C. Xu, C. Lei, L. Meng, C. Wang, and Y. Song, "Chitosan as a barrier membrane material in periodontal tissue regeneration," *Journal of Biomedical Materials Research B: Applied Biomaterials*, vol. 100, no. 5, pp. 1435–1443, 2012.

[2] S.-Y. Shin, H.-N. Park, K.-H. Kim et al., "Biological evaluation of chitosan nanofiber membrane for guided bong regeneration," *Journal of Periodontology*, vol. 76, no. 10, pp. 1778–1784, 2005.

[3] Y.-J. Yeo, D.-W. Jeon, C.-S. Kim et al., "Effects of chitosan nonwoven membrane on periodontal healing of surgically created one-wall intrabony defects in beagle dogs," *Journal of Biomedical Materials Research B: Applied Biomaterials*, vol. 72, no. 1, pp. 86–93, 2005.

[4] J.-S. Park, S.-H. Choi, I.-S. Moon, K.-S. Cho, J.-K. Chai, and C.-K. Kim, "Eight-week histological analysis on the effect of chitosan on surgically created one-wall intrabony defects in beagle dogs," *Journal of Clinical Periodontology*, vol. 30, no. 5, pp. 443–453, 2003.

[5] Q. X. Ji, J. Deng, X. M. Xing et al., "Biocompatibility of a chitosan-based injectable thermosensitive hydrogel and its effects on dog periodontal tissue regeneration," *Carbohydrate Polymers*, vol. 82, no. 4, pp. 1153–1160, 2010.

[6] M. N. V. Ravi Kumar, "A review of chitin and chitosan applications," *Reactive and Functional Polymers*, vol. 46, no. 1, pp. 1–27, 2000.

[7] P. K. Dutta, J. Duta, and V. S. Tripathi, "Chitin and chitosan: chemistry, properties and applications," *Journal of Scientific and Industrial Research*, vol. 63, no. 1, pp. 20–31, 2004.

[8] F. Croisier and C. Jérôme, "Chitosan-based biomaterials for tissue engineering," *European Polymer Journal*, vol. 49, no. 4, pp. 780–792, 2013.

[9] K. Madhumathi, K. T. Shalumon, V. V. D. Rani et al., "Wet chemical synthesis of chitosan hydrogel-hydroxyapatite composite membranes for tissue engineering applications," *International Journal of Biological Macromolecules*, vol. 45, no. 1, pp. 12–15, 2009.

[10] S. G. Caridade, E. G. Merino, N. M. Alves, and J. F. Mano, "Bioactivity and viscoelastic characterization of chitosan/bioglass composite membranes," *Macromolecular Bioscience*, vol. 12, pp. 1106–1113, 2012.

[11] Y. Zhang and M. Zhang, "Synthesis and characterization of macroporous chitosan/calcium phosphate composite scaffolds for tissue engineering," *Journal of Biomedical Materials Research*, vol. 55, no. 3, pp. 304–312, 2001.

[12] S. Pattnaik, S. Nethala, A. Tripathi, S. Saravanan, A. Moorthi, and N. Selvamurugan, "Chitosan scaffolds containing silicon dioxide and zirconia nano particles for bone tissue engineering," *International Journal of Biological Macromolecules*, vol. 49, no. 5, pp. 1167–1172, 2011.

[13] D. V. H. Thien, S. W. Hsiao, M. H. Ho, C. H. Li, and J. L. Shih, "Electrospun chitosan/hydroxyapatite nanofibers for bone tissue engineering," *Journal of Materials Science*, vol. 48, no. 4, pp. 1640–1645, 2013.

[14] S. Saravanan, S. Nethala, S. Pattnaik, A. Tripathi, A. Moorthi, and N. Selvamurugan, "Preparation, characterization and antimicrobial activity of a bio-composite scaffold containing chitosan/nano-hydroxyapatite/nano-silver for bone tissue engineering," *International Journal of Biological Macromolecules*, vol. 49, no. 2, pp. 188–193, 2011.

[15] W.-Y. Chuang, T.-H. Young, C.-H. Yao, and W.-Y. Chiu, "Properties of the poly(vinyl alcohol)/chitosan blend and its effect on the culture of fibroblast in vitro," *Biomaterials*, vol. 20, no. 16, pp. 1479–1487, 1999.

[16] Y. Zhang, X. Huang, B. Duan, L. Wu, S. Li, and X. Yuan, "Preparation of electrospun chitosan/poly(vinyl alcohol) membranes," *Colloid and Polymer Science*, vol. 285, no. 8, pp. 855–863, 2007.

[17] H. S. Mansur and H. S. Costa, "Nanostructured poly(vinyl alcohol)/bioactive glass and poly(vinyl alcohol)/chitosan/bioactive glass hybrid scaffolds for biomedical applications," *Chemical Engineering Journal*, vol. 137, no. 1, pp. 72–83, 2008.

[18] K. Lin, J. Chang, and R. Cheng, "In vitro hydroxyapatite forming ability and dissolution of tobermorite nanofibers," *Acta Biomaterialia*, vol. 3, no. 2, pp. 271–276, 2007.

[19] N. J. Coleman, "Aspects of the in vitro bioactivity and antimicrobial properties of Ag^{+}- and Zn^{2+}-exchanged 11 Å tobermorites," *Journal of Materials Science: Materials in Medicine*, vol. 20, no. 6, pp. 1347–1355, 2009.

[20] S.-H. Baek, H. Plenk Jr., and S. Kim, "Periapical tissue responses and cementum regeneration with amalgam, superEBA, and MTA as root-end filling materials," *Journal of Endodontics*, vol. 31, no. 6, pp. 444–449, 2005.

[21] S. Katsamakis, D. E. Slot, L. W. M. van der Sluis, and F. van der Weijden, "Histological responses of the periodontium to MTA: a systematic review," *Journal of Clinical Periodontology*, vol. 40, no. 4, pp. 334–344, 2013.

[22] T. Kokubo and H. Takadama, "How useful is SBF in predicting in vivo bone bioactivity?" *Biomaterials*, vol. 27, no. 15, pp. 2907–2915, 2006.

[23] E.-J. Lee, D.-S. Shin, H.-E. Kim, H.-W. Kim, Y.-H. Koh, and J.-H. Jang, "Membrane of hybrid chitosan-silica xerogel for guided bone regeneration," *Biomaterials*, vol. 30, no. 5, pp. 743–750, 2009.

[24] H. Shimauchi, E. Nemoto, H. Ishihata, and M. Shimomura, "Possible functional scaffolds for periodontal regeneration," *Japanese Dental Science Review*, vol. 49, no. 4, pp. 118–130, 2013.

[25] N. Patel, S. M. Best, W. Bonfield et al., "A comparative study on the in vivo behavior of hydroxyapatite and silicon substituted hydroxyapatite granules," *Journal of Materials Science: Materials in Medicine*, vol. 13, no. 12, pp. 1199–1206, 2002.

[26] I. D. Xynos, A. J. Edgar, L. D. K. Buttery, L. L. Hench, and J. M. Polak, "Gene expression profiling of human osteoblasts following treatment with the ionic dissolution products of Bioglass 45S5 dissolution," *Journal of Biomedical Materials Research*, vol. 55, no. 2, pp. 151–157, 2001.